Supporting Information for:

Screening of Bio-Compatible Metal-Organic Frameworks as Potential Drug Carriers using Monte Carlo Simulations

Maria C. Bernini,[a,b] *David Fairén-Jimenez,*[b,c,*] *Marcelo Pasinetti,*[a] *Antonio J. Ramirez-Pastor*[a] *and Randall Q. Snurr*[b]

[a]Departamento de Física, Instituto de Física Aplicada, Universidad Nacional de San Luis CONICET, San Luis, Argentina; [b]Department of Chemical and Biological Engineering, Northwestern University. Evanston, Illinois, United States and [c]Department of Chemical Engineering and Biotechnology, Pembroke St., University of Cambridge, Cambridge CB2 3RA, United Kingdom.

*Corresponding Author: df334@cam.ac.uk; http://people.ds.cam.ac.uk/df334

S1. Selected MOFs

MOFs for bio-medical applications must have a non-toxic composition. Regarding this, several factors need to be studied when a novel drug-carrier system is proposed. Indeed, two of them are critical: the toxicity and the daily requirement of the metal. To study the toxicity, it is common to consider the median lethal dose parameter, $LD_{50.}$ This parameter is defined as the amount of a compound that kills half the members of a tested population after a specific test duration. LD_{50} figures are frequently used as a general indicator of a substance's acute toxicity. In relation with the daily requirement, it is useful to quantify its biocompatibility.

Table S1. Oral LD_{50} in rats and daily requirements in humans of selected metals.[1]

Metal	LD_{50}*	Daily dose
	g/kg	mg
Zr	4.1	0.05
Ti	25	0.8
Cu	0.025	2
Mn	1.5	5
Fe	0.45	15
Zn	0.35	15
Mg	8.1	350
Ca	1.0	1000

*Oral LD50 for zirconyl acetate, titanium dioxide, copper(II) sulfate, manganese(II) chloride, iron(II) chloride, zinc chloride, magnesium chloride, calcium chloride.

We first selected three MOFs (MIL-53(Fe), MIL-100(Fe) and MIL-101(Cr)) that have been experimentally studied for drug delivery applications. The existence of experimental data[2] allowed us to validate our results. We then extended our study to three MOFs based on metals with acceptable (zinc, BioMOF-100) or high (magnesium, MOF-74(Mg); potassium, CDMOF-1(K)) bio-compatibility and low toxicity. The MOFs were also chosen to have a wide range of textural properties: MIL-53(Fe), MOF-74(Mg) and CDMOF-1(K) are microporous materials; MIL-100 and MIL-101 are mesoporous materials with microporous windows; BioMOF-100 is a strictly mesoporous MOF.

- **MIL-53(Fe),**[3] composed by $Fe^{(III)}$ and terephthalate ligand, is a flexible microporous MOF with 1D rhombic channels that can be opened or closed depending on the inclusion or absence of guest

molecules (Figure S1). MIL-53(Fe) exhibited a maximum uptake of 220 mg/g of ibuprofen and a total release achievable in 21 days.[2-b]

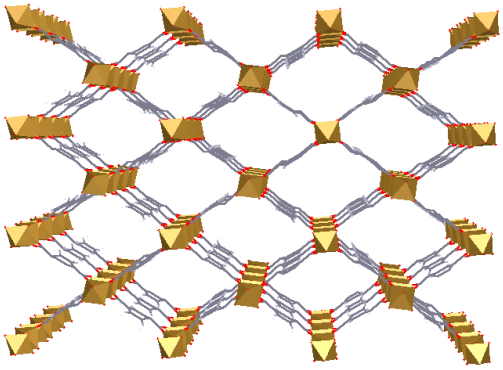

Figure S1. Projection of the crystal structure of MIL-53(Fe).

- **MIL-100(Fe)**,[4,5] composed by $Fe^{(III)}$ and 1,3,5-benzenetricarboxylate (BTC) ligand, is a rigid MOF with two different mesoporous spherical cages with diameters of *ca.* 25 and 29 Å (Figure S2-left), interconnected by pentagonal and hexagonal windows with diameters of *ca.* 5 Å and 8.5 Å, respectively. MIL-100(Fe) showed a maximum uptake of 330 mg/g and a time release of 3 days.[2-a]

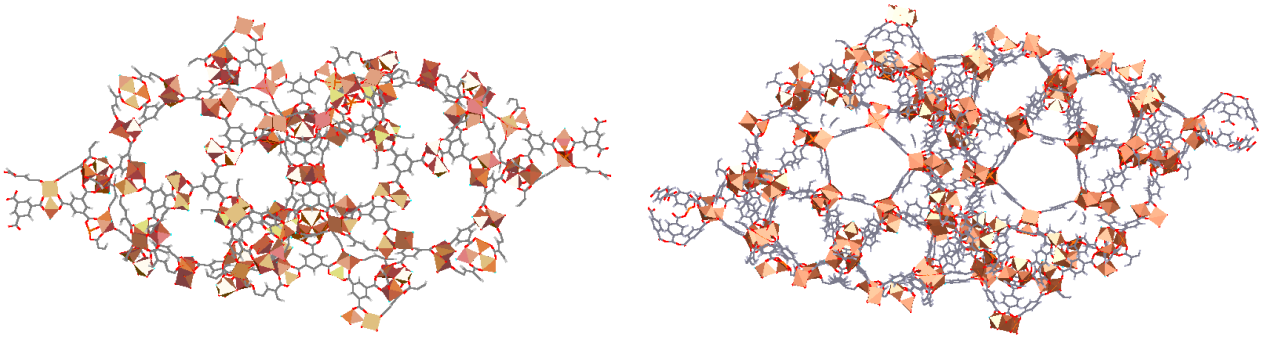

Figure S2. Projection of the crystal structures of (*left*) MIL-100 and (*right*) MIL-101.

- **MIL-101(Cr)**,[5] composed by $Cr^{(III)}$ and terephthalate ligand, is a rigid MOF with mesoporous spherical cages with diameters of *ca.* 25 Å and 34 Å (Figure S2-right). The cavities are accessible by pentagonal and hexagonal windows of 12 Å and 16 Å diameters, respectively. MIL-101(Cr) showed a record adsorption of 1376 mg/g, that is four and nine times higher than the adsorption achieved with mesoporous silica materials and zeolites, respectively.[8-a,d,9] Even though chromium is an extremely toxic metal, it has been included in this work as a proof of concept due to the experimental data available. Indeed, the homologous nontoxic iron MIL-101 exists.

- **MOF-74(Mg)**,[6] composed by 2,5-dihydroxyterephthalate and Mg(II) ion, is a microporous MOF with 1D hexagonal channels and 1D inorganic rod-shaped SBUs (Figure S3) that contains unsaturated open metal sites. It is interesting to note that the Mg(II) oral LD_{50} is the highest one (*i.e.* the lowest toxicity) among the more common metal ions used to prepare MOFs and its daily requirement is among the highest ones.

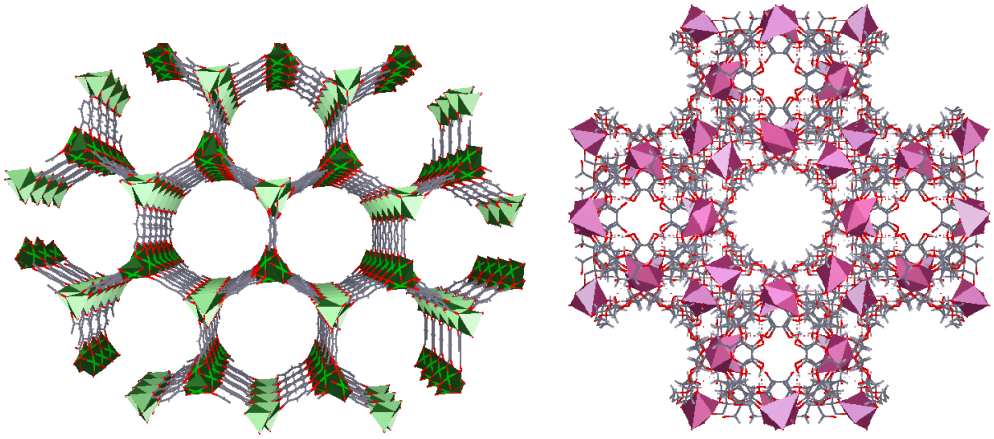

Figure S3. Projection of the crystal structure of (*left*) MOF-74 and (*right*) CDMOF-1.

- **CDMOF-1(K)**[7], is based on the edible precursors K^+ and γ-cyclodextrin (γ-CD, a symmetrical cyclic oligosaccharide that is mass-produced enzymatically from starch and is comprised of eight asymmetric α-1,4-linked D-glucopyranosyl residues). It consists of a cubic structure with γ-CD units located on the faces of the cube and assembled by K^+ ions, developing the porous, cationic 3D framework (Figure S3). The positive charge is compensated by free OH^- counter ions. Each K^+ ion is eight-coordinate, embracing two primary OH groups and two glycosidic ring oxygen atoms, as well as four secondary OH groups, all coming from the γ-CD tori. This MOF has cubic cavities of *ca.* 17 Å of diameter that are connected by cylindrical channels of *ca.* 7.8 Å in diameter, generating a 3D porous structure with a reported BET surface area of 1200 m^2/g.

- **BioMOF-100**[8] is composed of Zn-adeninate vertices linked by 4,4´-biphenyldicarboxylate ligands to develop a mesoporous MOF (Figure S4). It has an anionic framework, with four dimethylammonium (DMA) cations per formula unit compensating the charges. This MOF has an extremely high surface

area (about 4300 m^2/g), one of the lowest crystal densities (0.303 g cm^{-3}) and the largest pore volume (4.3 cm^3 g^{-1}) for a MOF, making it an outstanding candidate as a drug carrier. Furthermore, the toxicity and daily requirement of the Zn(II) ion are similar to those of Fe(II) ion.

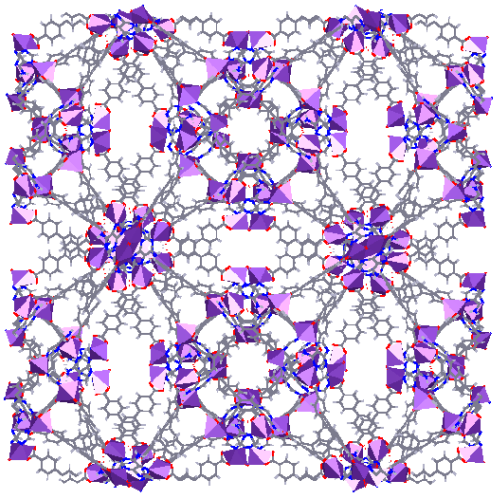

Figure S4. Projection of the crystal structure of BioMOF-100.

S2. Simulated ibuprofen adsorption isotherms

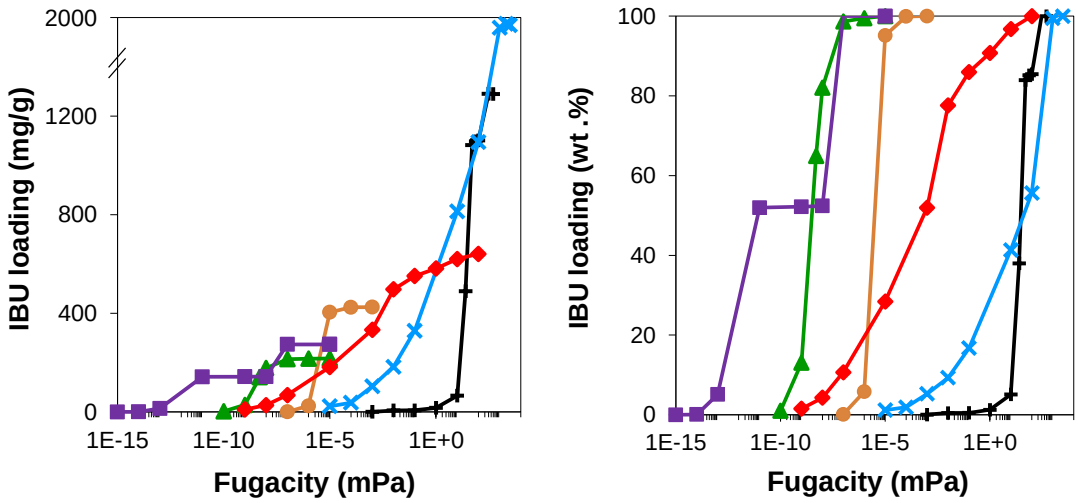

Figure S5. Simulated adsorption isotherms of IBU at 310 K (*left*) absolute and weight % normalized to their saturation value (*right*) for CDMOF-1, purple squares; MIL-53, green triangles; MOF-74, orange circles; MIL-100, red diamonds, BioMOF-100, blue crosses and MIL-101, black crosses. Error bars are smaller than the symbols.

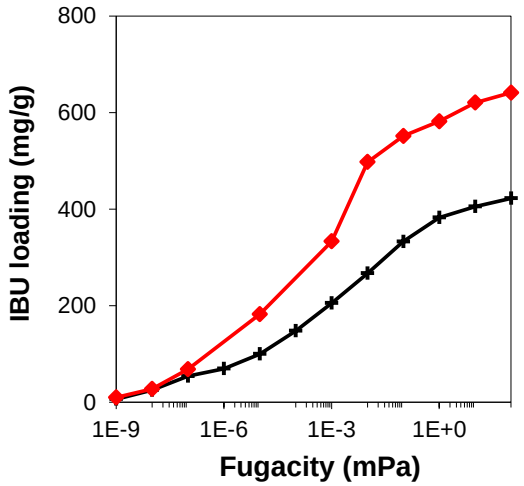

Figure S6. Simulated adsorption isotherms of IBU at 310 K in MIL-100, red diamonds. Black crosses represent the simulated adsorption isotherm with the narrower mesoporous cavities blocked.

S3. Simulation details

The adsorption of ibuprofen was investigated using grand canonical Monte Carlo (GCMC) simulations, performed with the multi-purpose code RASPA[9] at 310 K (*i.e.* 37 ˚C). We used an atomistic model for all MOF structures, in which the framework atoms were kept fixed at their crystallographic positions. Ibuprofen – ibuprofen and ibuprofen – framework interactions were calculated using a Lennard-Jones (LJ) + Coulomb potential. LJ parameters for the framework atoms were taken from the Universal Force Field (UFF).[10] No specific parameterization of the force field was used to simulate the interactions between the coordinatively unsaturated metal sites (e.g. Fe and Cr in MIL-100 and MIL-101, respectively). The use of generic force fields and a Coulomb potential has previously been shown to reproduce the adsorption mechanism of polar molecules such as CO_2, methanol and ionic liquids.[11] The ibuprofen molecule was constructed and modelled as flexible using the TraPPE force field[12] (Figure S8 and Table S3). Lorentz-Berthelot mixing rules were used for all cross terms, and LJ interactions beyond 12 Å were neglected. Coulomb interactions were calculated using partial charges on the atoms, obtained by a charge equilibration method.[13] The Ewald sum method was used to compute the electrostatic interactions. Up to 10^6 Monte Carlo equilibration cycles were performed plus 10^6 production cycles to calculate the ensemble averages. In one cycle, N moves were performed, where N is the number of molecules in the system, which fluctuates in GCMC. Monte Carlo moves used with equal probability were translation, rotation, insertion, deletion, random reinsertion, and regrowth of an existing molecule. Ibuprofen is a large molecule, so the fraction of successful insertions into the adsorbent can become too low. In order to speed up the convergence of the simulations, we used the configurational-bias Monte Carlo technique. This method is based on the Rosenbluth and Rosenbluth work[14], developed by a variety of researchers[15] and allows biasing the growth process of the flexible sections of the molecule towards energetically favourable configurations, reducing the overlap of the molecule with the framework atoms.

In the case of BioMOF-100, where dimethylammonium (DMA) cations are present inside the pores as counter ions, simulations to compute the siting of these cations were performed prior to the simulations with IBU. A model for rigid DMA cations was developed by optimizing the molecular geometry using the Forcite package implemented in Materials Studio[16] with the corresponding LJ parameters and partial charges taken from Nagy[17]. 96 DMA cations were inserted using a canonical ensemble Monte Carlo simulation on the empty framework. The positions of these cations were read at the beginning of the GCMC simulation of ibuprofen adsorption. Probabilities of rotation and translation of DMA cations were also included during the ibuprofen simulations.

The pore volume was obtained using a Widom particle insertion method, by probing the structure with a helium molecule at room temperature, recording a large number of random points not overlapping the van der Waals volume of the framework.[18] The pore size distributions were calculated using the method of Gelb and Gubbins,[19] where the largest sphere that can fit in a random point within a structure without overlapping the van der Waals surface of the framework is recorded for a large number of random points.

S4. MOF and ibuprofen models. Building blocks.

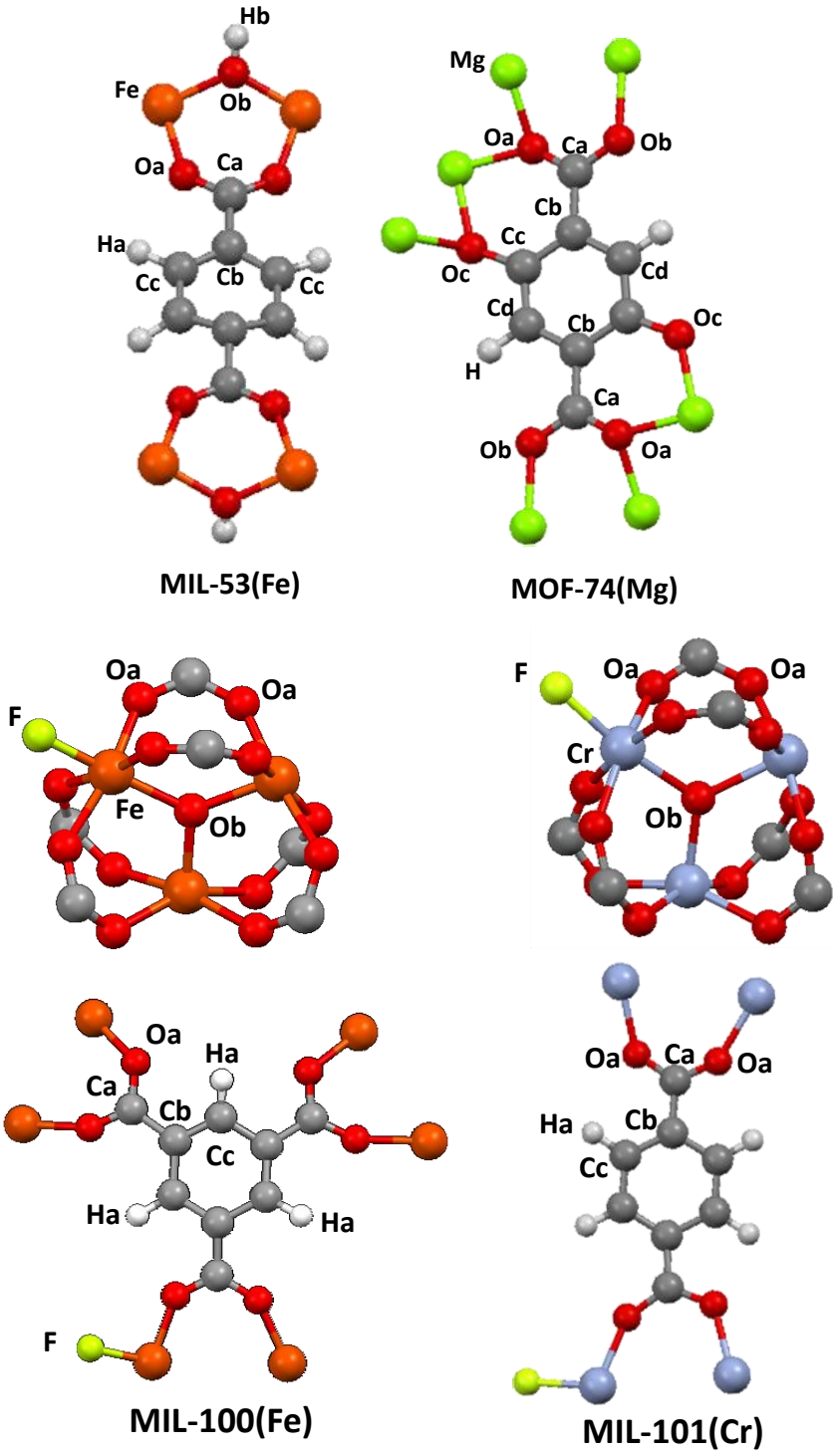

Figure S7. Cluster models of MIL-100(Fe), MIL-101(Cr), MIL-53(Fe) and MOF-74(Mg). The atom labels represent the atoms of the RDF analysis.

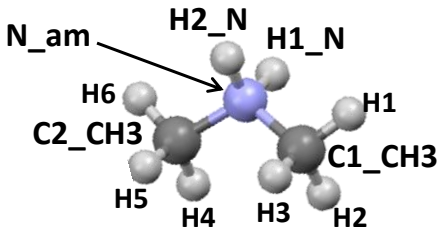

Dimethylammonium cation (DMA)

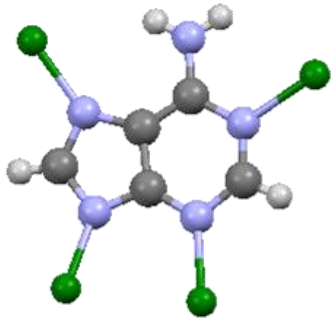

Zn-adeninate units

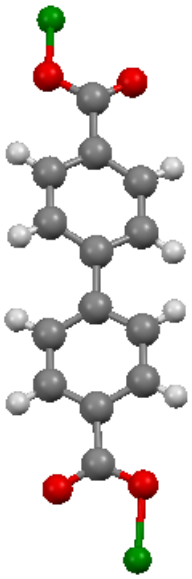

4,4´-bis(benzoate)

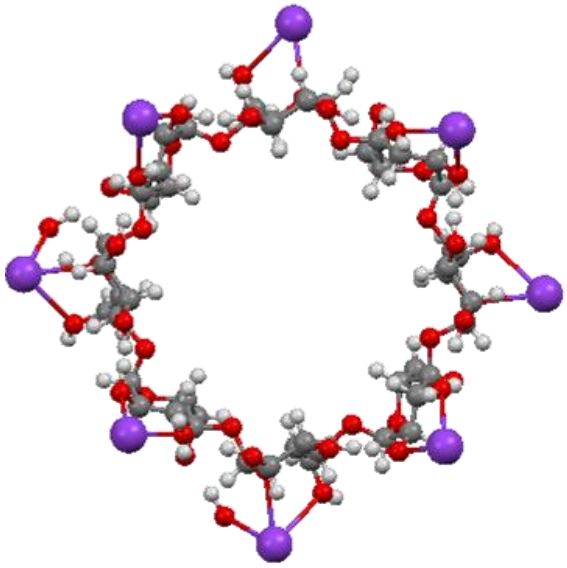

γ-CD tori in CDMOF-1(K)

Figure S8. (*top*) Building blocks of BioMOF-100 and (*bottom*) γ-CD tori ring in CDMOF-1(K). Color-atom codes: Mof_C: gray; Mof_O: red, Mof_N: light-blue; Mof_Zn: green, Mof_H: white; Mof_K: light-purple, these atom labels represent the atoms of the RDF analysis.

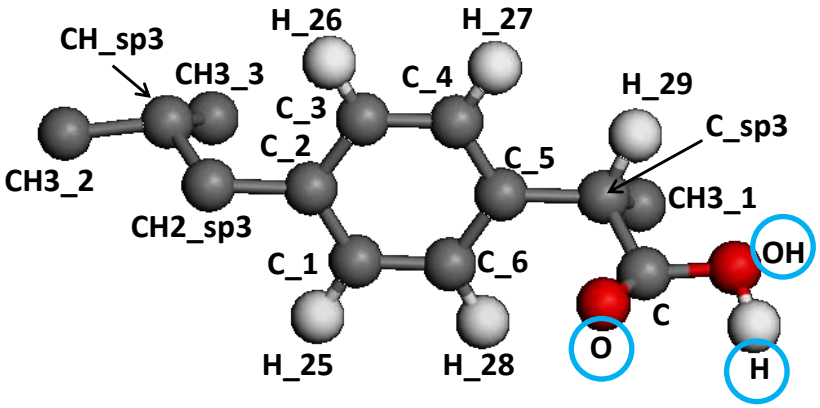

Figure S9. Ibuprofen model used during the GCMC simulations. Highlighted in blue, the atoms used to obtain the RDF (Figures S10-S16)

S5. Force Field Parameters

The ibuprofen molecule was constructed and modeled as flexible using the TraPPE force field.[11] LJ parameters for framework atoms were taken from the Universal Force Field (UFF)[20]. In all simulations, MOFs were modeled as rigid, using the crystallographic available data. Bending and torsional movements for the IBU molecules were calculated according to the following potentials:

Harmonic Bend

$$U = \tfrac{1}{2}p_0\left(\theta_{ijk} - p_1\right)^2$$

where p_0/k_B in units K/rad^2, p_1 in degrees.

TRAPPE Dihedral

$$U = p_0 + p_1[1 + \cos(\phi_{ijkl})] + p_2[1 - \cos(2\phi_{ijkl})] + p_3[1 + \cos(3\phi_{ijkl})]$$

where p_0/k_B, p_1/k_B, p_2/k_B, p_3/k_B in units K.

Three Cosine Dihedral

$$U = \tfrac{1}{2}p_0[1 + \cos(\phi_{ijkl})] + \tfrac{1}{2}p_1[1 - \cos(2\phi_{ijkl})] + \tfrac{1}{2}p_2[1 + \cos(3\phi_{ijkl})]$$

where p_0/k_B, p_1/k_B, p_2/k_B in units of K.

Harmonic Improper Dihedral

$$U = \frac{1}{2}p_0\left(\phi_{ijkl} - p_1\right)^2$$

where p_0/k_B in units K/rad^2, p_1 in degrees.

CFF Dihedral

$$U = p_0[1 - \cos\left(\phi_{ijkl}\right)] + p_1\,[1 - \cos\left(2\phi_{ijkl}\right)] + p_2[1 + \cos\left(3\phi_{ijkl}\right)]$$

where p_0/k_B, p_1/k_B, p_2/k_B, p_3/k_B in units K.

Table S2. Lennard-Jones parameters for the framework atoms. Atom labels are according with the models presented in Figures S7 and S8.

	Sigma Å	**Epsilon/k K**
	MIL-53(Fe)	
Ha	22.141	2.572
Hb	22.141	2.572
Fe	6.542	2.594
Oa	30.192	3.119
Ob	30.192	3.119
Ca	52.836	3.431
Cb	52.836	3.431
Cc	52.836	3.431
	MIL-100(Fe)	
Ha	22.141	1 2.572
F	25.161	2.997
Fe	6.542	2.594
Oa	30.192	3.119
Ob	30.192	3.119
Ca	52.836	3.431
Cb	52.836	3.431
Cc	52.836	3.431
	MIL-101(Cr)	
Ha	22.141	2.572
F	25.161	2.997
Cr	7.548	2.693
Oa	30.192	3.119
Ob	30.192	3.119
Ca	52.836	3.431
Cb	52.836	3.431
Cc	52.836	3.431

Table S2 (*cont.*). Lennard-Jones parameters for the framework atoms. Atom labels are according with the models presented in Figures S7 and S8.

	Sigma **Å**	**Epsilon** **K**
MOF-74(Mg)		
Mg	55.855	2.692
Ca	52.836	3.431
Cb	52.836	3.431
Cc	52.836	3.431
Cd	52.836	3.431
H	22.141	2.572
Oa	30.192	3.119
Ob	30.192	3.119
Oc	30.192	3.119
CDMOF-1(K)		
Mof_C	52.836	3.431
Mof_O	30.192	3.119
Mof_H	22.141	2.572
Mof_K	17.612	3.397
BioMOF-100		
Mof_Zn	62.397	2.462
Mof_O	30.192	3.119
Mof_C	52.836	3.431
Mof_H	22.141	2.572
Mof_N	34.721	3.261
C1_CH3	33.213	3.5
C2_CH3	33.213	3.5
N_am	85.549	3.25
H1_N	0	0
H2_N	0	0
H_1	15.097	2.5
H_2	15.097	2.5
H_3	15.097	2.5
H_4	15.097	2.5
H_5	15.097	2.5
H_6	15.097	2.5

Table S3. Lennard-Jones Parameters and partial charges for ibuprofen atoms. Atom labels are according with the models presented in Figures S7 and S8.

Label	Pseudo atom	Sigma Å	Epsilon K	Charge e
1	C_5	30.7	3.60	0.114
2	C_6	30.7	3.60	-0.127
3	C_1	30.7	3.60	-0.124
4	C_2	30.7	3.60	0.132
5	C_3	30.7	3.60	-0.126
6	C_4	30.7	3.60	-0.118
7	H_28	25.45	2.36	0.081
8	H_25	25.45	2.36	0.081
9	H_26	25.45	2.36	0.083
10	H_27	25.45	2.36	0.106
11	C_sp3	0.50	6.40	-0.188
12	CH2_sp3	46.00	3.95	-0.054
13	CH3_1	98.00	3.75	0.050
14	H_29	15.30	3.31	0.114
15	C	41.00	3.90	0.590
16	O	79.00	3.05	-0.471
17	OH	93.00	3.02	-0.489
18	H	0.00	0.00	0.320
19	CH_sp3	10.00	4.68	0.043
20	CH3_2	98.00	3.75	-0.008
21	CH3_3	98.00	3.75	-0.009

Table S4. Ibuprofen bond definitions and bond distances.

Label		Type of bond	Bond distance
1	2		Å
4	12	FIXED_BOND	1.514
1	11	FIXED_BOND	1.528
11	13	FIXED_BOND	1.538
11	14	FIXED_BOND	1.105
11	15	FIXED_BOND	1.523
15	16	FIXED_BOND	1.213
15	17	FIXED_BOND	1.354
17	18	FIXED_BOND	0.972
12	19	FIXED_BOND	1.555
19	20	FIXED_BOND	1.534
19	21	FIXED_BOND	1.534

* Labels correspond to definition of pseudo atom types given in Table S3

Table S5. Ibuprofen angle definitions and bending vibration parameters.

Label*			Type of potential	P_0	P_1
1	**2**	**3**		**K/rad^2**	**°**
16	15	17	HARMONIC_BEND	40300	123.0
15	17	18	HARMONIC_BEND	17600	107.0
17	15	11	HARMONIC_BEND	35300	111.0
16	15	11	HARMONIC_BEND	40300	126.0
13	11	1	HARMONIC_BEND	62500	112.0
1	11	15	HARMONIC_BEND	187500	114.0
13	11	15	HARMONIC_BEND	62500	114.0
14	11	15	HARMONIC_BEND	18883	110.7
14	11	1	HARMONIC_BEND	18883	110.7
14	11	13	HARMONIC_BEND	18883	110.7
4	12	19	HARMONIC_BEND	375000	114.0
12	19	20	HARMONIC_BEND	62500	112.0
12	19	21	HARMONIC_BEND	62500	112.0
21	19	20	HARMONIC_BEND	62500	112.0

* Labels correspond to definition of pseudo atom types given in Table S3.

Table S6. Ibuprofen dihedral angles definitions and potential parameters.

Label				Type of potential	Parameters			
1	**2**	**3**	**4**		**p0**	**p1**	**p2**	**p3**
18	17	15	16	TRAPPE_DIHEDRAL	0	630	781.2	0
17	15	11	1	THREE_COSINE_DIHEDRAL	710.06	-136.38	1582.64	
17	15	11	13	THREE_COSINE_DIHEDRAL	710.06	-136.38	1582.64	
17	15	11	14	THREE_COSINE_DIHEDRAL	710.06	-136.38	1582.64	
16	15	11	13	TRAPPE_DIHEDRAL	0	630	781.2	0
18	17	15	11	TRAPPE_DIHEDRAL	0	630	781.2	0
16	15	11	1	TRAPPE_DIHEDRAL	2035.58	-736.9	57.84	-293
13	11	1	6	TRAPPE_DIHEDRAL	688.5	86.63	-109.77	-282.24
13	11	1	2	TRAPPE_DIHEDRAL	688.5	86.63	-109.77	-282.24
20	19	12	4	TRAPPE_DIHEDRAL	-251.06	428.73	-111.85	441.27
21	19	12	4	TRAPPE_DIHEDRAL	-251.06	428.73	-111.85	441.27
19	12	4	5	TRAPPE_DIHEDRAL	688.5	86.63	-109.77	-282.24
19	12	4	3	TRAPPE_DIHEDRAL	688.5	86.63	-109.77	-282.24
11	1	6	9	HARMONIC_IMPROPER_DIHEDRAL	24800	180		
11	1	2	7	HARMONIC_IMPROPER_DIHEDRAL	24800	180		
9	5	6	10	HARMONIC_IMPROPER_DIHEDRAL	24800	180		
8	3	2	7	HARMONIC_IMPROPER_DIHEDRAL	24800	180		
1	6	5	9	HARMONIC_IMPROPER_DIHEDRAL	26800	0		
1	2	3	8	HARMONIC_IMPROPER_DIHEDRAL	26800	0		
4	5	6	10	HARMONIC_IMPROPER_DIHEDRAL	26800	0		
4	3	2	7	HARMONIC_IMPROPER_DIHEDRAL	26800	0		
16	15	11	14	CFF_DIHEDRAL	0	0	854	
14	11	1	2	CFF_DIHEDRAL	0	0	854	
14	11	1	6	CFF_DIHEDRAL	0	0	854	

* Labels correspond to definition of pseudo atom types given in Table S3. Parameters for each potential type are defined in Section S5.

S6. Radial distribution functions (RDF)

In this section, the RDF involving the most important anchoring points of the adsorbents and the IBU molecules is presented. For each pair of atom, RDF at different IBU loadings (expressed as the % of weight normalized to their saturation values) is displayed. Atom labels are according to definitions given in Section S4 (see above).

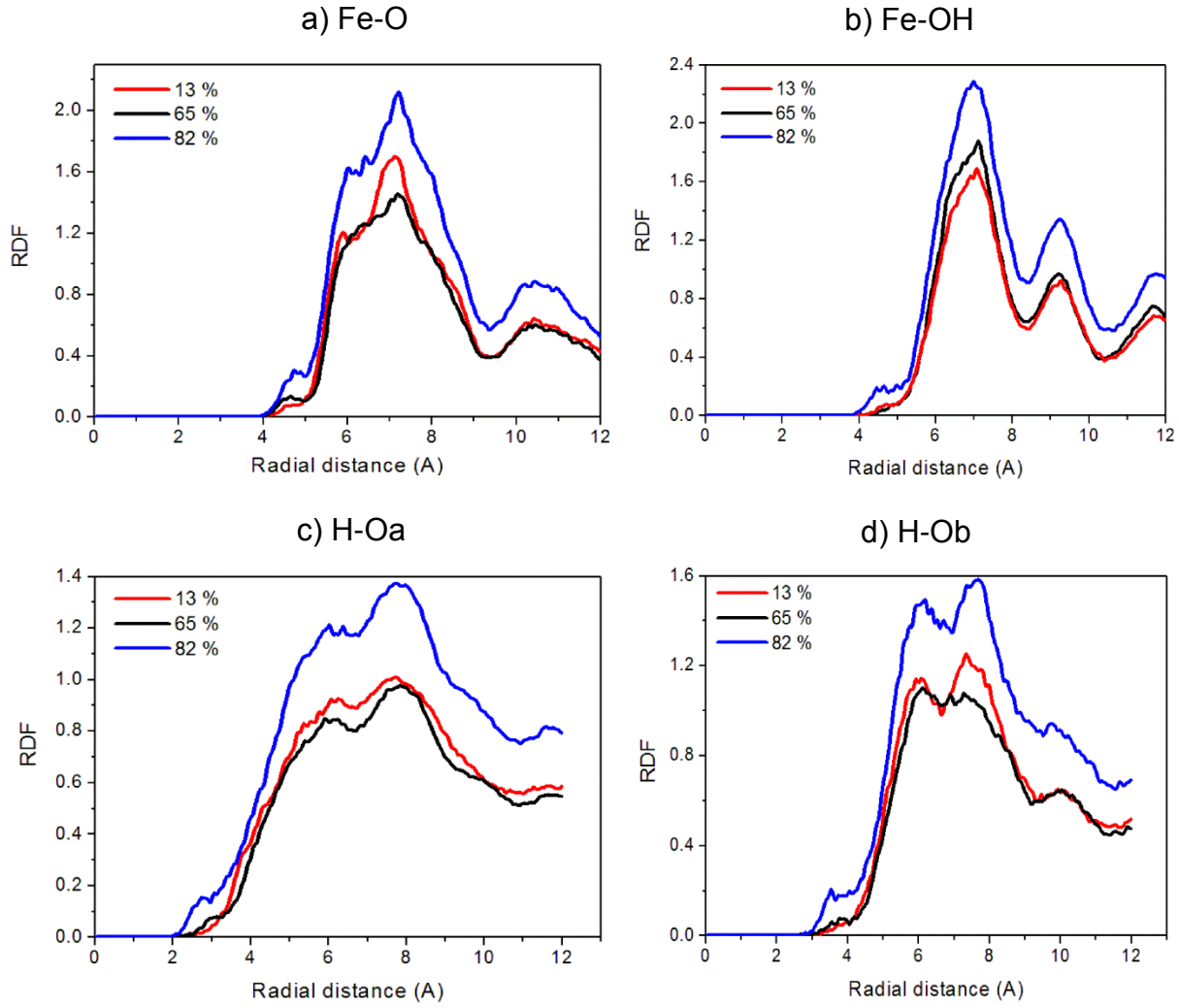

Figure S10. Radial distribution functions, RDF, obtained from a simulated isotherm of ibuprofen on MIL-53 at 310 K and different normalized IBU loadings (indicated as % of saturation). RDF shows the interactions involving the framework Fe atoms and the carboxylic group atoms O and OH (Figure S9) of IBU (*a*,*b*) and the H-bonds between the hydrogen atom of the carboxylic group of IBU, H in Figure S9 (as donors) and the framework oxygen atoms (as acceptors) (c, d). Labels are according with models displayed in Section S4.

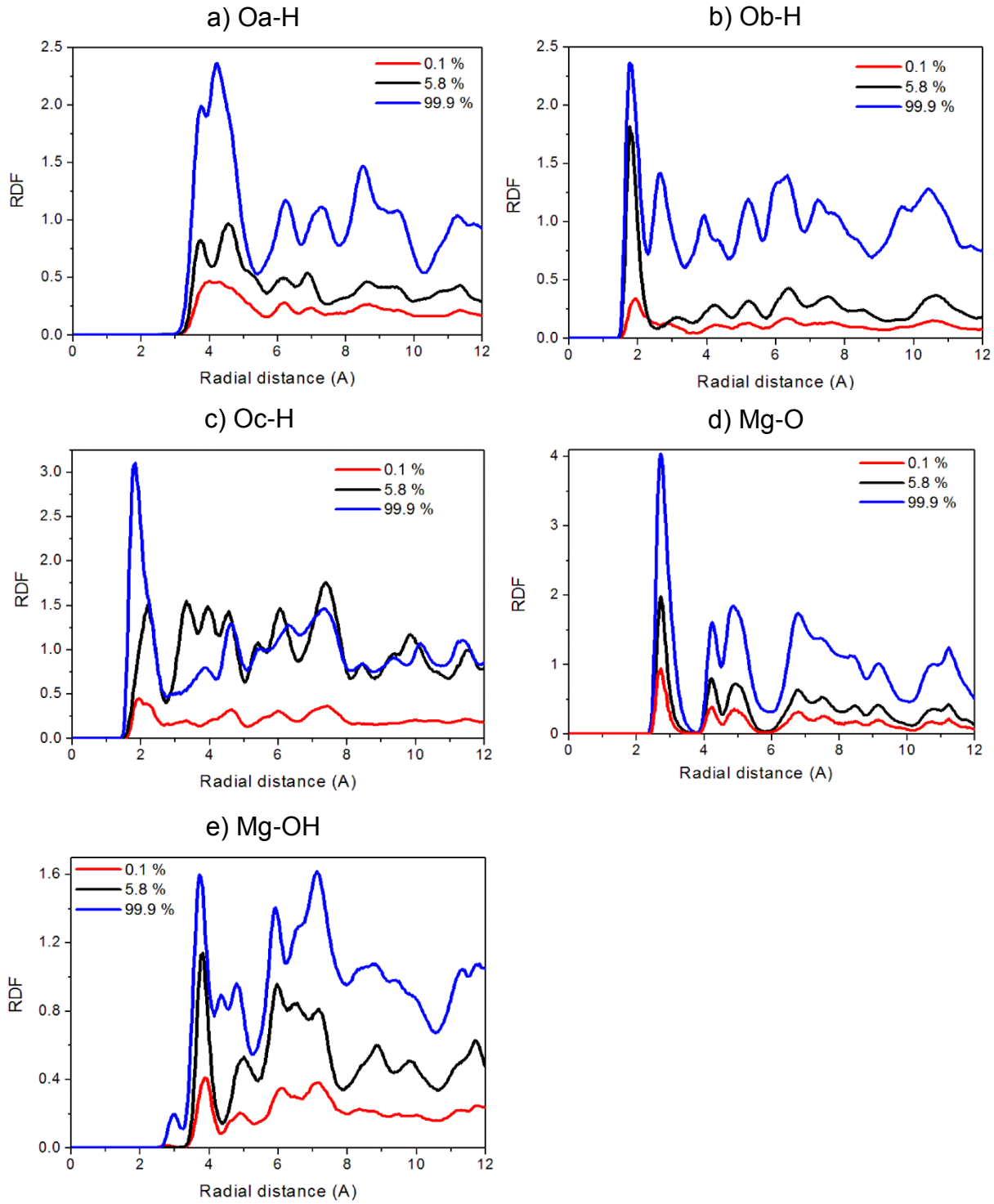

Figure S11. RDF obtained from a simulated isotherm of ibuprofen on MOF-74(Mg) at 310 K and different normalized IBU loadings (indicated as % of saturation). RDF shows the H-bond interactions between the framework oxygen atoms Oa, Ob and Oc and the hydrogen atom of the carboxylic group of IBU (H in Figure S9) (*a*-*c*) and the interactions between the coordinatively unsaturated Mg(II) ion and the carboxylic group atoms O and OH of IBU (*d*,*e*). Labels are according with models displayed in Section S4.

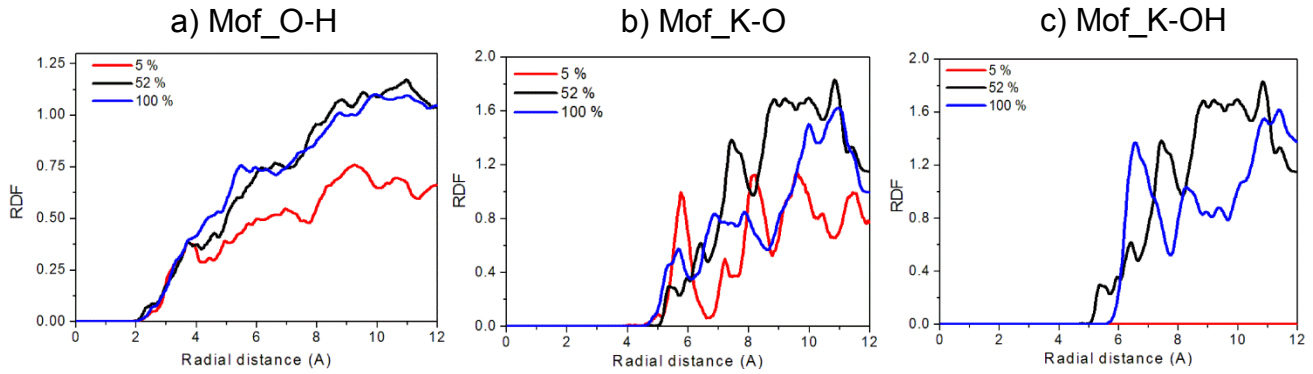

Figure S12. RDF obtained from a simulated isotherm of ibuprofen on CDMOF-1 at 310 K and different normalized IBU loadings (indicated as % of saturation). RDF shows the H-bonds between the framework oxygen atoms (as acceptors) and the hydrogen atom of the carboxylic group of IBU (as donor) (*a*) and the interactions between the framework potassium ions and the carboxylic group atoms O and OH of IBU (*b*,*c*). Labels are according with models displayed in Section S4.

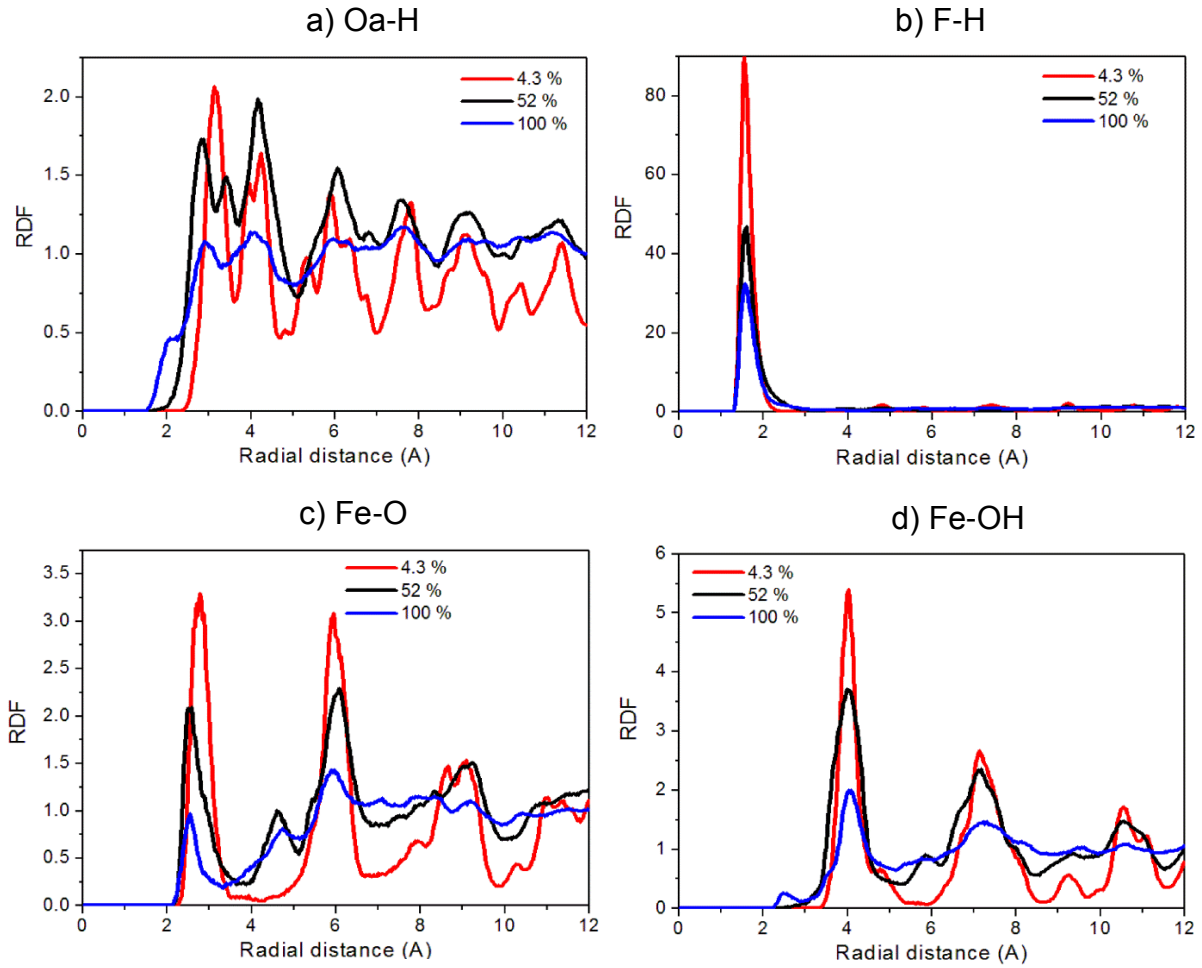

Figure S13. RDF obtained from a simulated isotherm of ibuprofen on MIL-100 at 310 K and different normalized IBU loadings (indicated as % of saturation). RDF shows the H-bonds between the framework oxygen atoms Oa (*a*) and the coordinated fluorine atoms (*b*) with the hydrogen atom of the carboxylic group of IBU, and the interactions between the Fe(III) and the carboxylic group atoms O and OH of IBU (*c*,*d*). Labels are according with models displayed in Section S4.

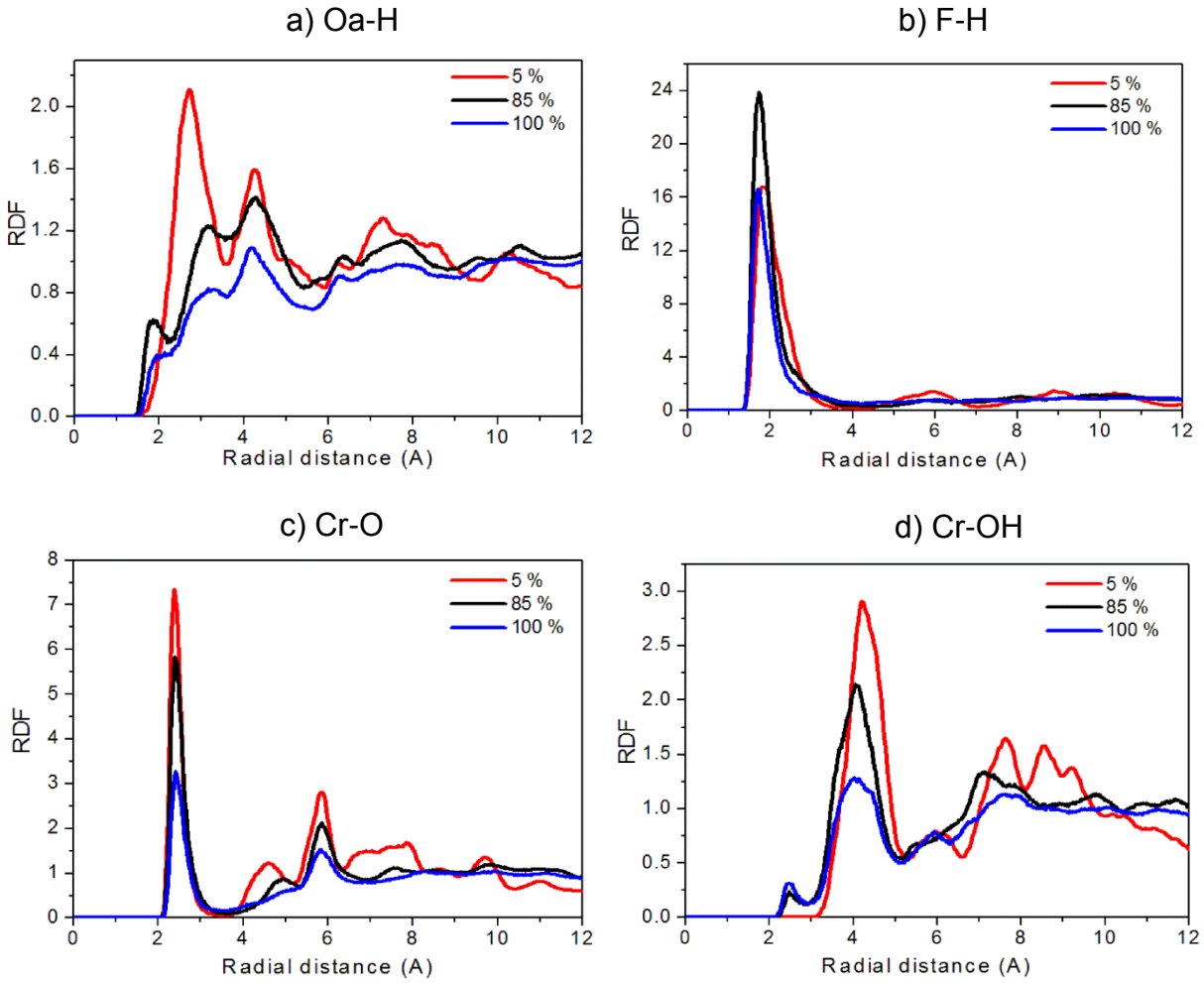

Figure S14. RDF obtained from a simulated isotherm of ibuprofen on MIL-101 at 310 K and different normalized IBU loadings (indicated as % of saturation). RDF shows the H-bonds between the framework oxygen Oa (*a*) and fluorine (*b*) atoms with the hydrogen atom of the carboxylic group of IBU, and the interactions between the Cr(III) ions and the carboxylic group atoms O and OH of IBU (*c*,*d*).). Labels are according with models displayed in Section S4.

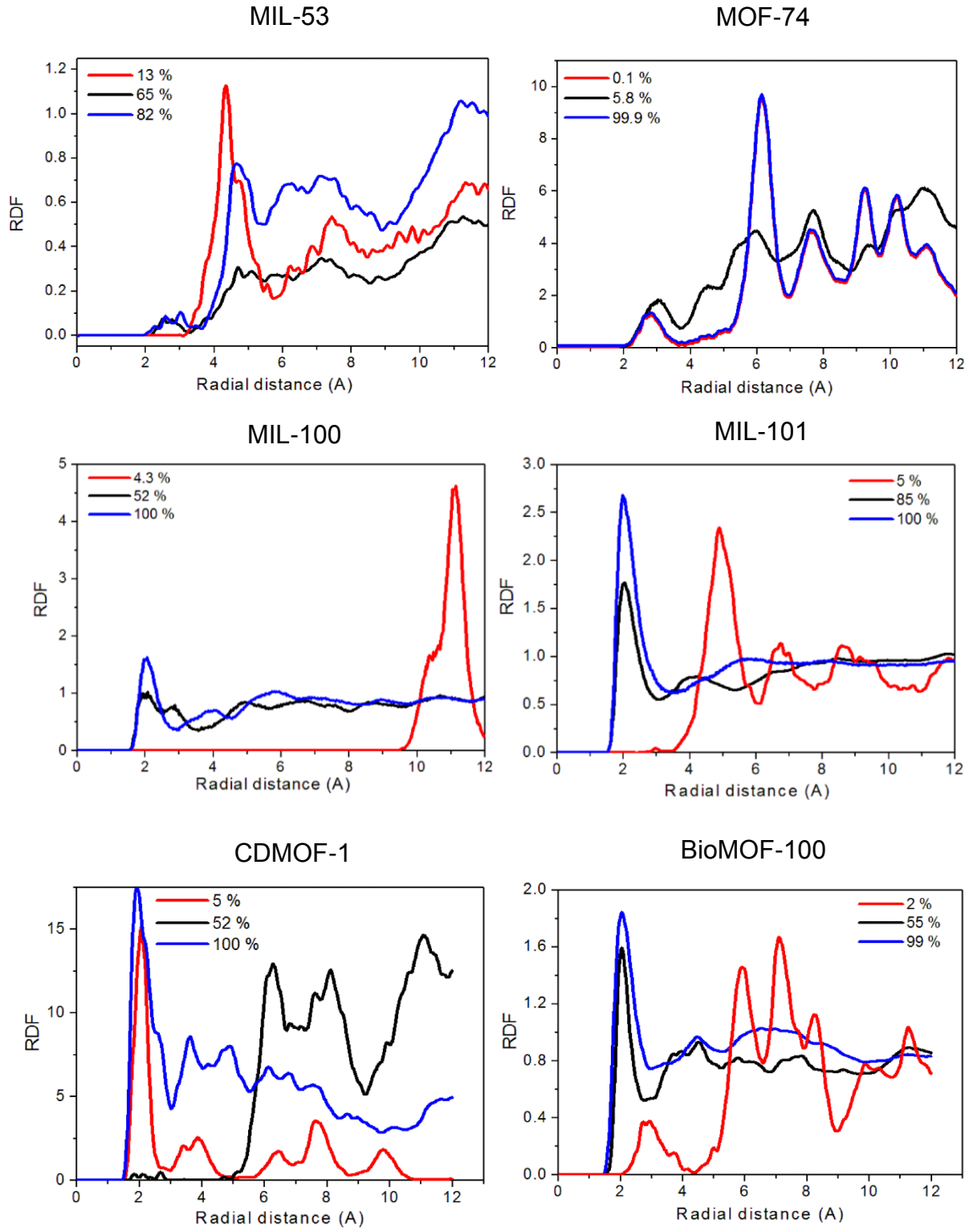

Figure S15. RDF of H-bond interaction involving carboxylic groups (O-framework and H-IBU atoms, see Figure S9) of different adsorbed IBU molecules in the six different MOFs.

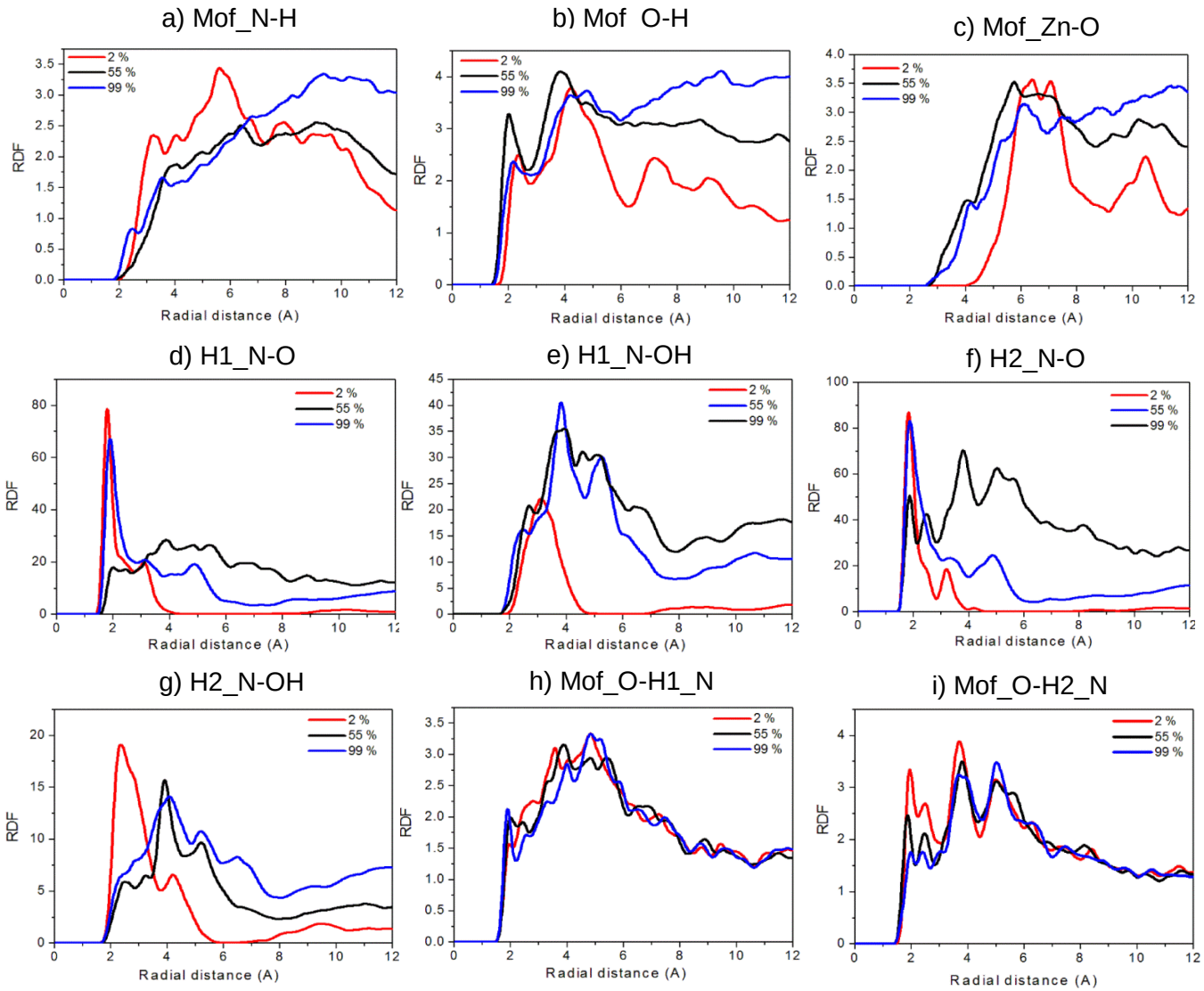

Figure S16. RDF obtained from a simulated isotherm of ibuprofen on BioMOF-100 at 310 K and different normalized IBU loadings (indicated as % of saturation). RDF shows interactions involving the most important anchoring points between frameworks atoms (Mof_N, Mof_ Mof_O and Mof_Zn) and the carboxylic atoms H (*a, b)* and O *(c)* of IBU, trimethylammonium atoms (H1_N and H2_N) and IBU oxygen atoms (O and OH) (*e-g*) and framework oxygen atoms (Mof_O) and trimethylammonium atoms (H1_N and H2_N) (*h,i*). Labels are according with models displayed in Section S4.

S7. Snapshots

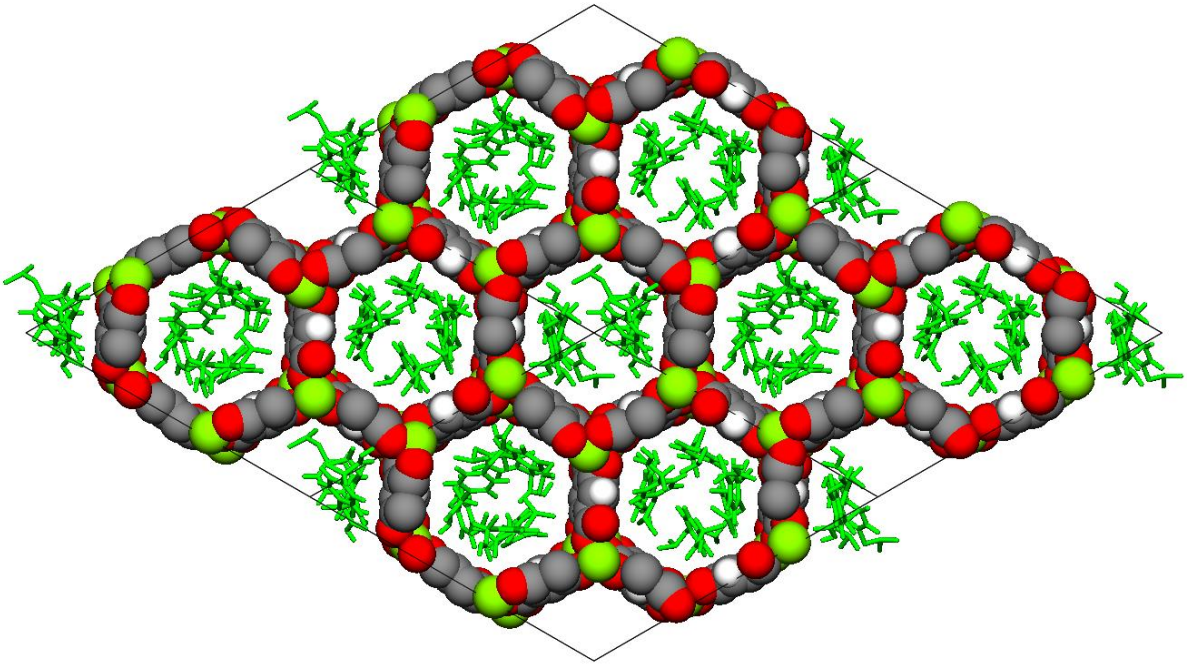

Figure S17. Snapshots of ibuprofen in MOF-74(Mg) at saturation, showing 2×2×4 unit cells. Ibuprofen molecules are shown in green stick-mode.

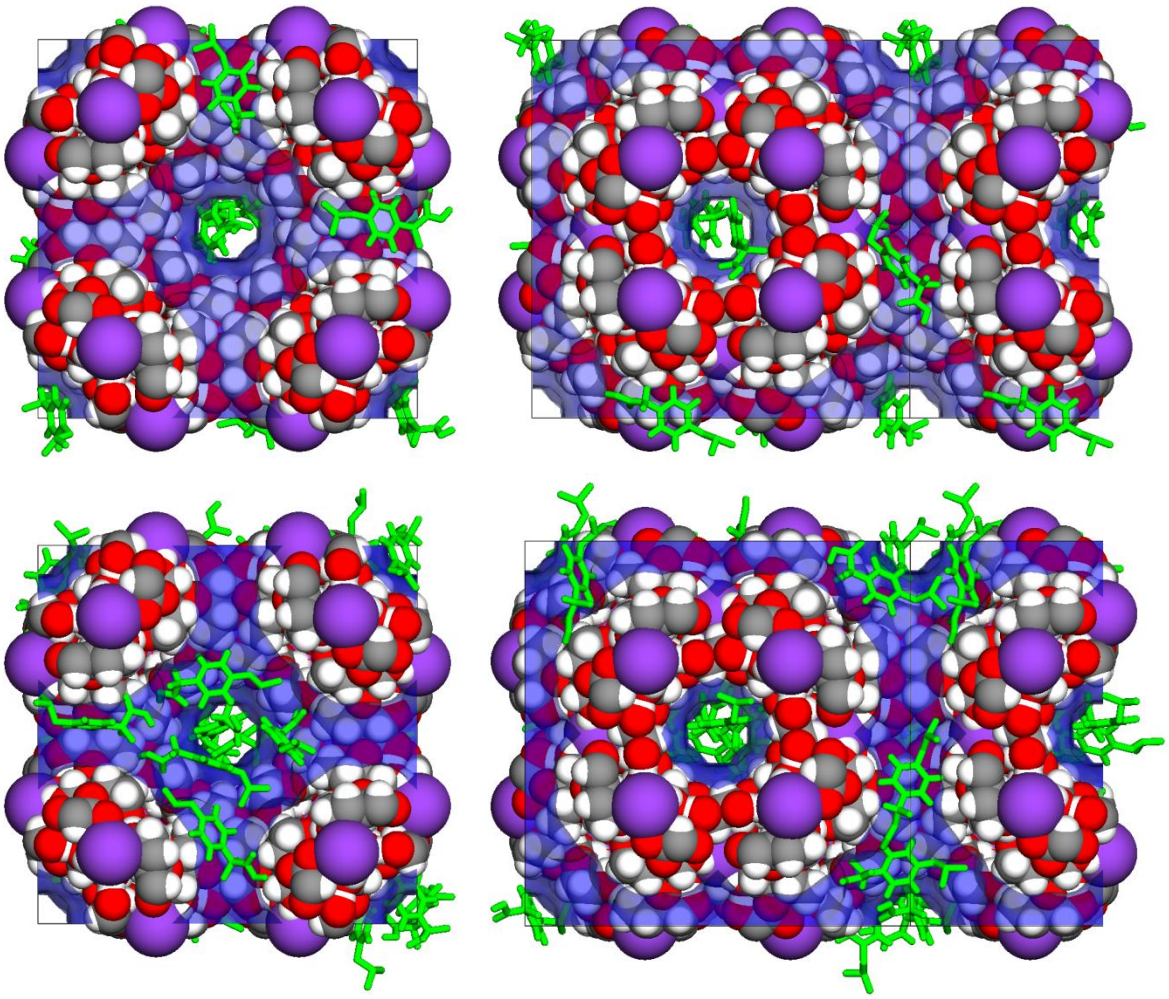

Figure S18. Snapshots of adsorbed ibuprofen molecules in CDMOF-1 at different loadings: (*top*) 143 mg/g and (*bottom*) 274 mg/g. Ibuprofen molecules are shown in green stick-mode. The accessible surface is shown in blue.

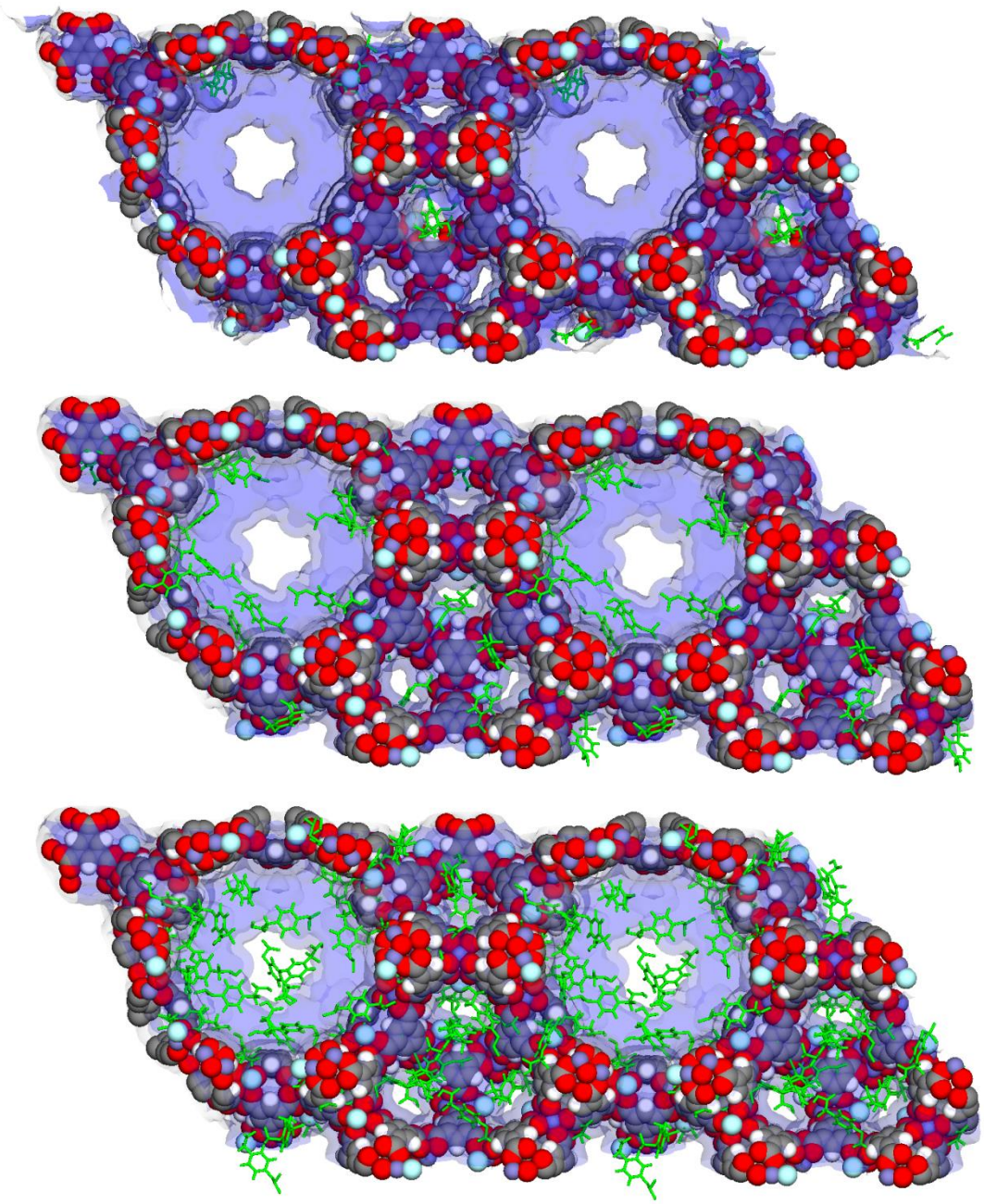

Figure S19. Snapshots of ibuprofen in MIL-100 at different uptakes: (*top*) 68 mg/g, (*center*) 333 mg/g and (*bottom*) 641 mg/g. Only a slice of the structure has been represented for clarity. Ibuprofen molecules are shown in green stick-mode. The accessible surface is shown in blue.

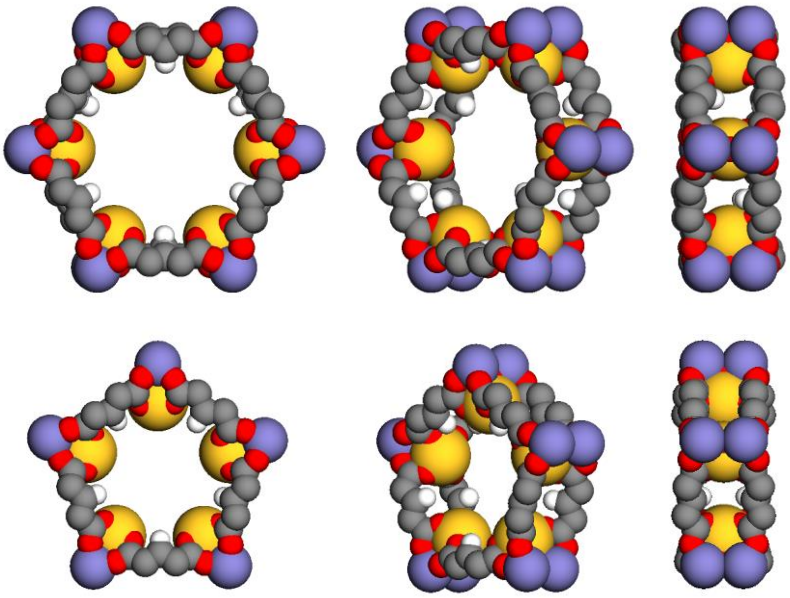

Figure S20. Detail of the hexagonal and pentagonal windows in MIL-100. Coordinatively unsaturated Fe sites, pointing to the centre of the windows, are highlighted in yellow. Only a fraction of the linker atoms have been represented for clarity.

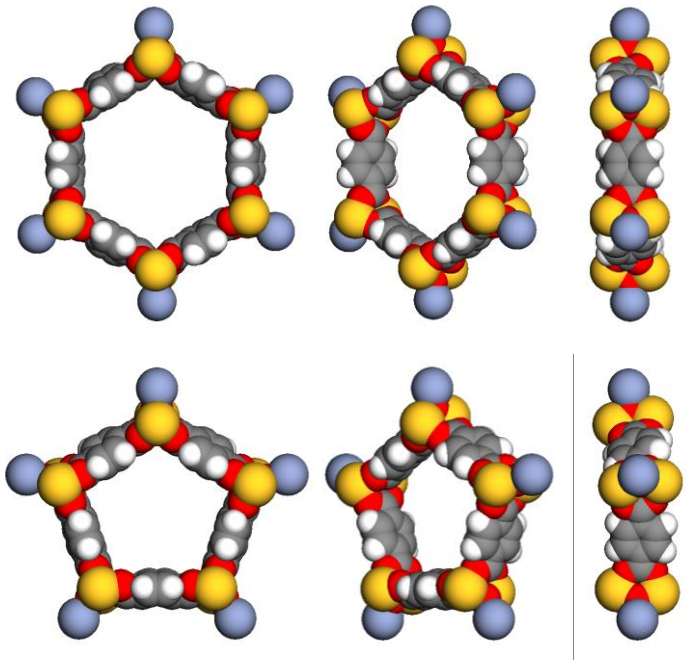

Figure S21. Detail of the hexagonal and pentagonal windows in MIL-101. Coordinatively unsaturated Cr sites, pointing to the centre of the cavities, are highlighted in yellow.

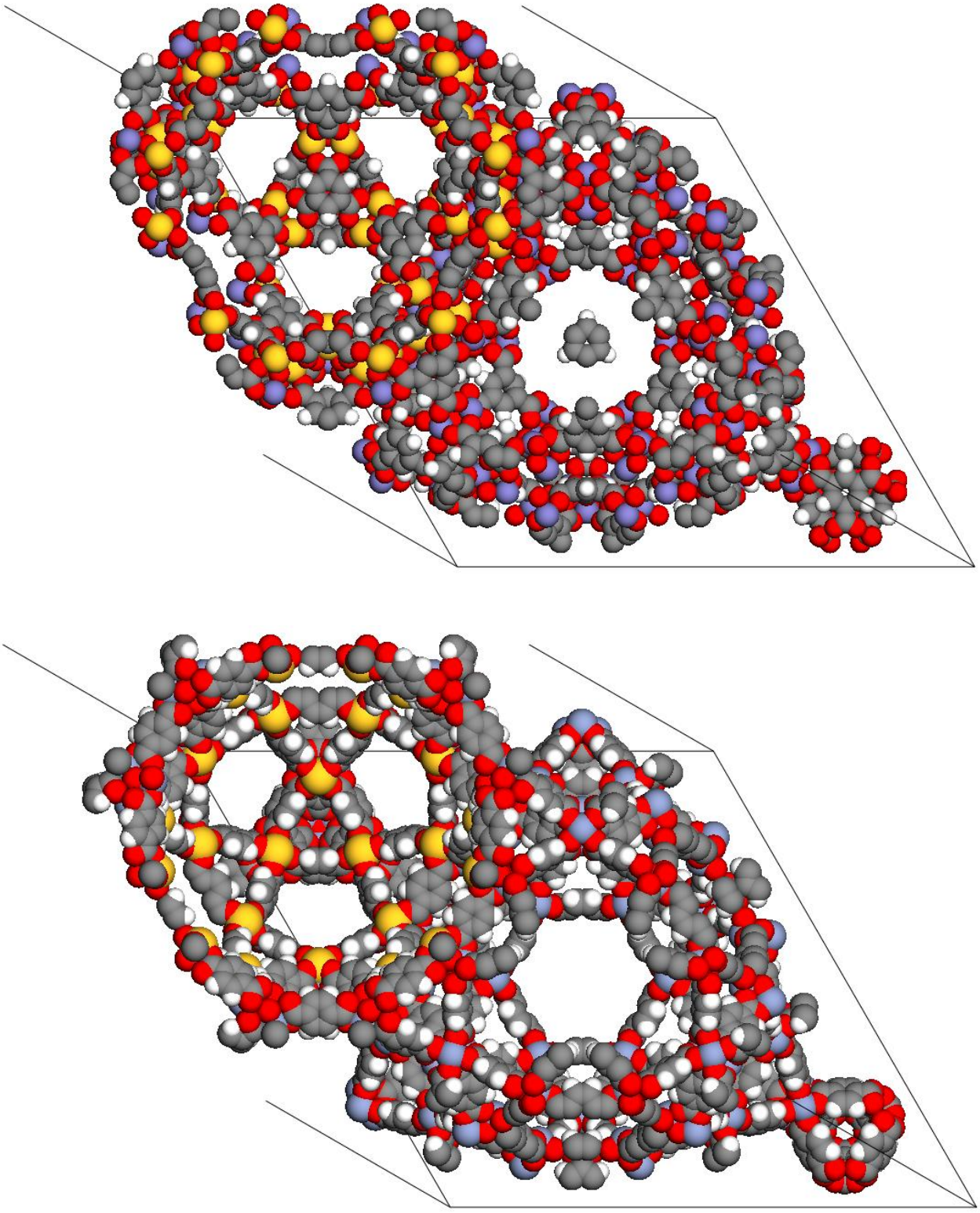

Figure S22. Representation of the (*top*) MIL-100 and (*bottom*) MIL-101 structures. Coordinatively unsaturated metal sites of one cavity have been highlighted in yellow. Note that Cr (MIL-101) is pointing to the centre of the cavities.

S8. References

[1] Horcajada, P.; Gref, R.; Baati, T.; Phoebe, T.; Allan, K.; Maurin, G.; Couvreur, P.; Ferey, G.; Morris, R.E.; Serre, C. *Chem. Rev.* ***2012***, 112, 1232–1268

[2] a) Horcajada, P.; Serre, C.; Vallet-Regi, M.; Sebban, M.; Taulelle, F.; Ferey, G. *Angew. Chem., Int. Ed*. **2006**, 45, 5974-5978; b) Horcajada, P.; Serre, C.; Maurin, G.; Ramsahye, N. A.; Balas, F.; Vallet-Regi, M.; Sebban, M.; Taulelle, F.; Ferey, G. *J. Am. Chem. Soc.* **2008**, 130, 6774-6780.

[3] Whitfield, T. R.; Wang, X.; Liu, L.; Jacobson, A. *J. Solid State Sci*. **2005**, 7, 1096-1103.

[4] a) Férey, G.; Serre, C.; Mellot-Draznieks, C.; Millange, F.; Surblé, S. *Angew. Chem.* **2004**, 116, 6456-6461; *Angew. Chem. Int. Ed.* **2004**, 43, 6296-6301.

[5] Ferey, G.; Mellot-Draznieks, C.; Serre, C.; Millange, F.; Dutour, J.; Surble, S.; Margiolaki, I. *Science* **2005**, 309, 2040-2042.

[6] Dietzel, P. D. C.; Blom, R.; Fjellvag, H. *Eur. J. Inorg. Chem.* **2008**, 23, 3624-3632.

[7] a) Smaldone, R. A.; Forgan, R. S.; Furukawa, H.; Gassensmith, J. J.; Slawin, A. M. Z.; Yaghi, O. M.; Stoddart, J. F. *Angew. Chem., Int. Ed*. **2010**, 49, 8630-8634; b) Forgan, R. S.; Smaldone, R. A.; Gassensmith, J. J.; Furukawa, H.; Cordes, D. B.; Li, Q.; Wilmer, C. E.; Botros, Y. Y.; Snurr, R. Q.; Slawin, A. M. Z.; Stoddart J.F. *J Am. Chem. Soc*. **2012**, 134, 406–417.

[8] An, J.; Farha, O. K.; Hupp, J.T.; Pohl, E.; Yeh, J. I.; Rosi, N. L. *Nature Communications*, **2012**, 3, 604, 1-6.

[9] Dubbeldam, D.; Calero, S.; Ellis, D. E.; Snurr, R. Q. RASPA 1.0; Northwestern University: Evanston, IL, 2008.

[10] Rappé, A. K., Casewit, C. J., Colwell, K. S., Goddard III, W. A. & Skiff, W. M. *J. Am. Chem. Soc.* **1992**, 114, 10024-10035.

[11] a) Castillo, J. M.; Vlugt, T. J. H.; Calero, S. *J. Phys. Chem. C*, **2008**, *112* (41), 15934–15939; b) Gutiérrez-Sevillano, J.J.; Vicent-Luna, J. M.; Dubbeldam, D.; Calero, S. *J. Phys. Chem. C*, **2013**, *117* (21), 11357–11366.

[12] a) Rai, N.; Siepmann, J. I. *J. Phys. Chem. B* **2007**, 111, 10790-10799; b) Clifford, S. Bolton, K., Ramjugernath, D. *J. Phys. Chem. B* **2006**, 110, 21938-21943; c) Stubbs, J. M.; Potoff, J.J.; Siepmann, J. I. *J. Phys. Chem. B* **2004**, 108, 17596-17605; d) Wick, C.D.; Martin, M.G.; Siepmann, J.I. *J. Phys. Chem. B* **2000**, 104, 8008-8016; e) Martin, M.G.; Siepmann, J.I. *J. Phys. Chem. B* **1999**, 103, 4508-4517; f) Wick, C.D.; Stubbs, J.M.; Rai, N.; Siepmann; I.I. *J. Phys. Chem. B* **2005**, 109, 18974-18982.

[13] Wilmer, C. E.; Kim, K.C.; Snurr, R. Q. *J. Phys. Chem. Lett*. **2012**, 3, 2506−2511.

[14] Rosenbluth, M. N.; Rosenbluth, A. W. *J. Chem. Phys.* **1955**, 23, 356.

[15] a) J. Harris, S.A. Rice. *J. Chem. Phys*. **1988**, 88(2), 1298-1307; b) J.I. Siepmann. *Mol. Phys.*, **1990**, 70(6), 1145-1158; c) J.I. Siepmann and D. Frenkel. *Mol. Phys*., 1992, 75(1), 59-70; d) D. Frenkel, G.C.A.M. Mooij, B. Smit. *J. Phys.: Condens. Matter*. **1992**, 4(12), 3053-3076; e) J.J. de Pablo, M. Suter, U.W. Suter. J. Chem. phys. **1992**, 96, 2395-2403; f) M. Laso, J.J. de Pablo, and U.W. Suter. J. Phys.: Condens. Matter. **1992**, 97(4), 2817-2819; g) J.I. Siepmann and I.R. McDonald. *Mol. Phys.* **1992**, 75(2), 255-259.

[16] Materials Studio v6.1. Accelrys Software Inc., San Diego, CA 92121, USA.

[17] Nagy, P. I. *Phys. Chem. Chem. Phys*., **2012**, 14, 849–857.

[18] a) Arif Nadeem, M.; Thornton, A. W.; Hill, M. R.; Stride, J. A. *Dalton Trans*. **2011**, 40, 3398-3401; b) Krishna, R.; van Baten, J. M. *Phys. Chem. Chem. Phys.* **2011**, 13, 10593-10616; c) Mayo, S. L.; Olafson, B. D.; Goddard III, W. A. *J. Phys. Chem.* **1990**, 94, 8897-8909; d) Duren, T.; Millange, F.; Ferey, G. ; Walton, K. S.; Snurr, R. Q.; *J. Phys. Chem. C* **2007**, 111, 15350-15356; e) Myers, A. L. Thermodynamics of Adsorption, in Chemical Thermodynamics for Industry, ed. T. M. Letcher, Royal Society of Chemistry, Cambridge, 2004.

[19] Gelb, L. D.; Gubbins, K. E. *Langmuir*, 1998, 15, 305-308.

20 Rappé, A. K., Casewit, C. J., Colwell, K. S., Goddard III, W. A. & Skiff, W. M. *J. Am. Chem. Soc.* 114, 10024-10035 (1992).